PHILOSOPHICAL TRANSACTIONS OF THE ROYAL SOCIETY A
MATHEMATICAL, PHYSICAL & ENGINEERING SCIENCES

Kinematics of Fault Creep

C.-Y. King, R. D. Nason and D. Tocher

Phil. Trans. R. Soc. Lond. A 1973 **274**, 355-360
doi: 10.1098/rsta.1973.0063

Phil. Trans. R. Soc. Lond. A. **274**, 355–360 (1973) [355]
Printed in Great Britain

Kinematics of fault creep

By C.-Y. King, R. D. Nason and D. Tocher
Earthquake Mechanism Laboratory, National Oceanic and Atmospheric Administration, San Francisco, California 94105, *U.S.A.*

Fault slip and strain during fault-creep episodes are continuously recorded by a dense network of creepmeters deployed along several major traces of the San Andreas fault system in central California. These data are analysed on the basis of theoretical faulting models to delineate the kinematics of the fault-creep process. The results indicate that fault creep is a failure propagation phenomenon, kinematically similar to seismic faulting, but with very low characteristic rates. The speed of creep propagation is not constant and is of the order of 10 km/day or less. The maximum slip velocity usually ranges from 0.1 to 10 μm/s. Both of these are five or more orders of magnitude smaller than the corresponding rates of seismic faulting. The slowness in particle motion can account for the ineffectiveness of the creep process in exciting observable seismic waves. However, the tectonic strain released by a creep event may be sizable. The largest event recorded so far has a rupture length of 6 km and a maximum offset of 9 mm, comparable to similar parameters of a shallow earthquake of magnitude 4.7.

Introduction

Slippage along a tectonic fault may occur violently to generate earthquakes or gradually in a little understood process called fault creep (Steinbrugge & Zacher 1960). Early instrumental studies of fault creep by Tocher (1960) at the Cienega Winery in California indicated that the creep motion of the San Andreas fault occurred there largely in episodes of relatively short duration (a few millimetres offset in several days) separated by long intervals (months) during which little or no slip took place. Subsequent measurements at the Winery and other locations showed that creep was widely occurring along San Andreas, Calaveras and Hayward faults in central California (Nason 1971) and that creep episodes at two sites near each other sometimes began at somewhat different times, suggesting that creep might be a failure propagation process (Nason 1970). The apparent speed of creep propagation along the fault trace was estimated to be about 1 to 10 km/day (Nason 1970) and the maximum slip velocity ranged between 0.1 to 10 μm/s (King, Nason & Tocher 1970), both of which are roughly five or more orders of magnitude smaller than the corresponding rates of seismic faulting. King *et al.* (1970) found that some gross features of the creep records matched the expectations from a theoretical faulting model by King (1970). They inferred that a large creep event might have a rupture zone several kilometres long and an offset of perhaps as much as a few centimetres.

In order to study the creep kinematics in more detail, it is important to record an event with several closely spaced creepmeters. To this end, the Earthquake Mechanism Laboratory (E.M.L.) of the U.S. National Oceanic and Atmospheric Administration (N.O.A.A.) has, over the past few years, gradually built up a dense network of creepmeters in central California. This network has now recorded a large number of creep events, some on two or more creepmeters. This paper reports on some recent results of observation and analysis, which, as will be shown later, generally agree with the earlier approximate estimates.

Fault-creep data

Figure 1 shows the distribution of the N.O.A.A.–E.M.L. creepmeters in California. The creepmeters, described by Nason (1971), use an invar rod 3 mm in diameter and are typically 15 m long spanning the fault trace at a 45° angle. One end of the rod is fixed rigidly to an anchor pier and the other is loosely tensioned by a spring attached to an instrument pier. Fault slip causes a change in distance between the two piers. This change is sensed with a potentiometer and is recorded continuously on a strip-chart recorder with a resolution of 0.1 mm and a chart speed of 6 mm/h. A creepmeter also functions as a strainmeter of low sensitivity (10^{-5} to 10^{-6}).

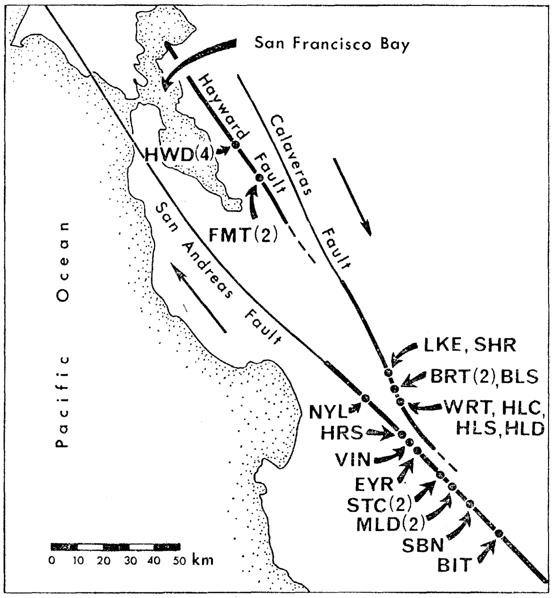

Figure 1. Distribution of N.O.A.A.–E.M.L. creepmeters on San Andreas, Calaveras, and Hayward faults in central California. The fault motion in this region is right-lateral strike slip, ranging from 0 to 3 cm/year in recent years.

Figure 2 shows creep records (direct tracing of originals, showing offset as function of time) of three events, each recorded on two creepmeters on the San Andreas fault. The first event began at Harris Ranch (HRS) on 30 July 1970 but did not reach Cienega Winery (VIN) 4 km away until 9 h later. The apparent speed of propagation is 11 km/day, which is somewhat higher than the speed of 7 km/day for an earlier event at the same stations (Nason 1970). The other two events in figure 2 were recorded at Melendy Ranch (MLD) where two creepmeters with a common timer were placed only 0.17 km apart. The apparent propagation speeds are approximately 80 and 20 km/day respectively. The difference in the apparent speed may be due mainly to geometric effects. These effects cannot be isolated without more recording stations.

On 17 July 1971 a large event occurred within an array of six creepmeters along the Hayward–Calaveras fault (figure 3*b*). This event was recorded on the four middle creepmeters over a 5.0 km stretch, but not on the two creepmeters at the ends, 6.8 km apart. Thus the rupture length of the event can be directly determined to be 5.9 ± 0.9 km. A maximum offset of 9 mm was recorded at WRT. The apparent creep propagation speed showed a relatively high initial value of 24 km/day. The speed decreased considerably near the end of the event.

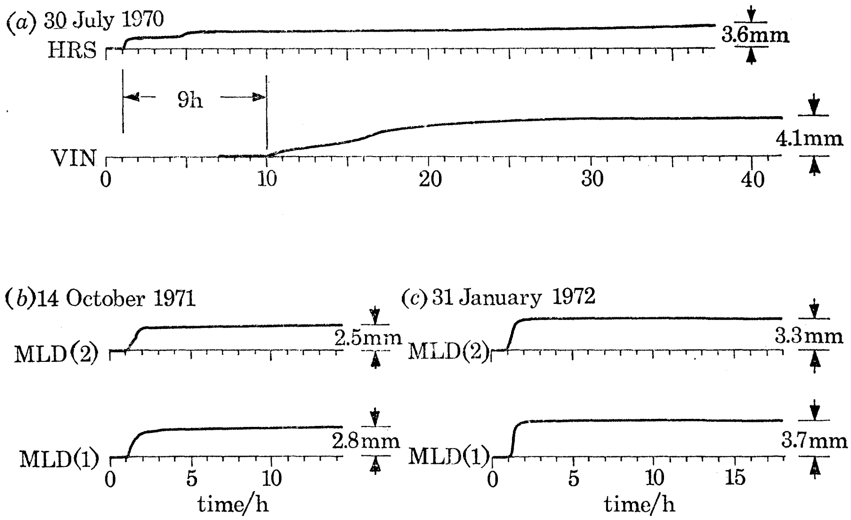

Figure 2. Three creep events, each recorded by two creepmeters on San Andreas fault. (*a*) $\Delta x = 4.0$ km; $\Delta t_0 = 9.0$ h; $\Delta x/\Delta t_0 = 11$ km/day. (*b*) $\Delta x = 0.17$ km; $\Delta t_0 = 3$ min; $\Delta x/\Delta t_0 = 80$ km/day. (*c*) $\Delta x = 0.17$ km; $\Delta t_0 = 13$ min; $\Delta x/\Delta t_0 = 20$ km/day. Here Δx is distance between creepmeters and Δt_0, time difference between the beginnings of creep episodes. The ratio $\Delta x/\Delta t_0$ is apparent propagation speed along the fault trace.

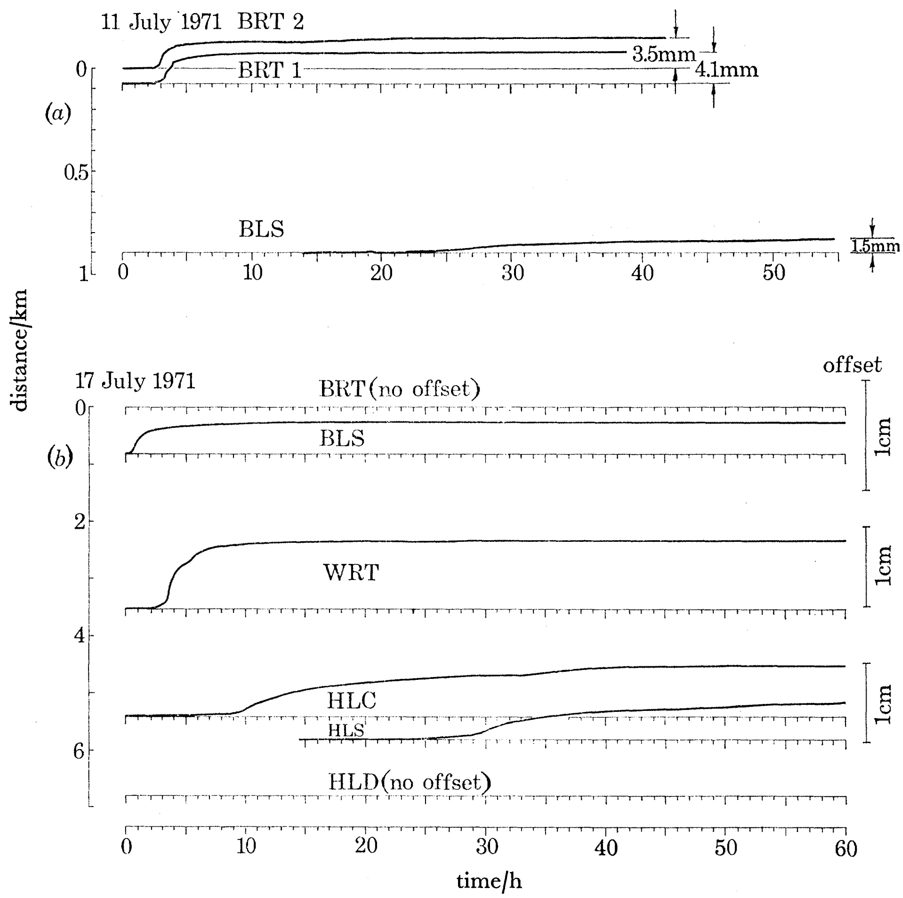

Figure 3. Two creep events that occurred within a dense array of creepmeters on the Hayward–Calaveras fault. The records are arranged properly in both time and space except for station BRT (2) whose timer was out of order.

Six days before the large event, a smaller one occurred immediately to the north and was recorded on a creepmeter in common (BLS, figure 3*a*). It may be considered as a *fore-creep* event, in analogy to a foreshock of an earthquake.

The slip velocities of the creep events may be obtained from the slopes of the creep curves. Their maximum values usually fall in the range of 0.1 to 10 μm/s as in previously recorded events.

Analysis

The creep data can be analysed on the basis of a theoretical faulting model by King (1972). In this model, rupture starts at a point at a shallow depth and spread on a vertical fault plane with a circular boundary. The centre of curvature of the boundary, called the *guiding centre*,

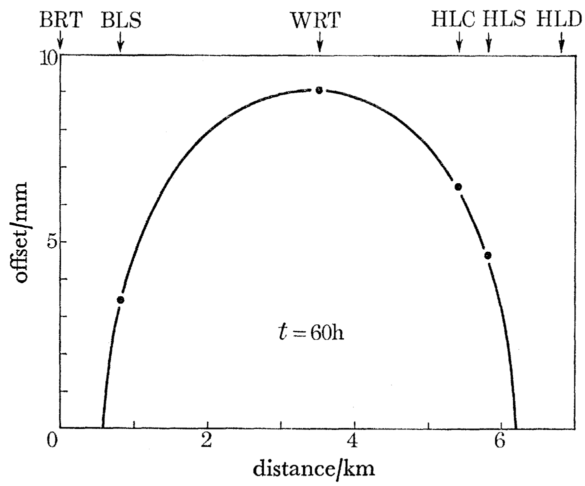

FIGURE 4. The 17 July 1971 creep event has an elliptical distribution of offset along the fault at the end of the episode.

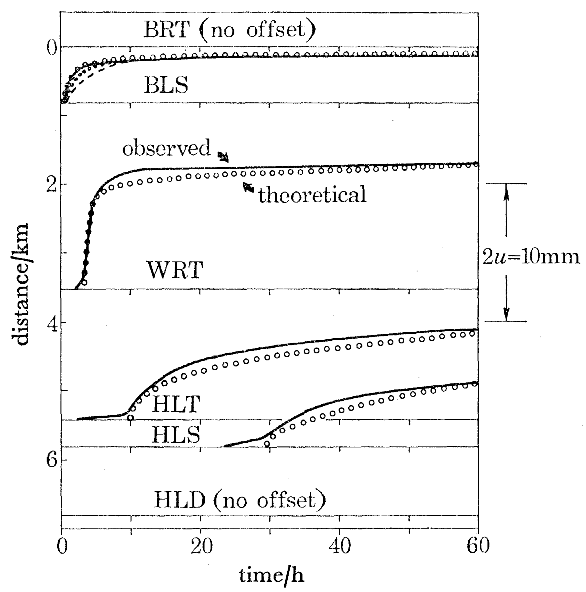

FIGURE 5. Theoretical and observed creep curves for the 17 July 1971 event. Shown are results of three models whose guiding centres move in a horizontal direction at three different depths: ○, h = 0 km; ●, h = 0.5 km; –, h = 1.0 km. The model curves are significantly different only at BLS. $2u$ is offset.

moves in a prescribed path while the *guiding radius* expands. King (1972) showed several cases where the offset has a cosine distribution function of a constant shape of the guiding radius.

The observed final offsets of the 17 July 1971 event fit an elliptical distribution with a maximum-offset to rupture–length ratio of 1.6×10^{-6} (figure 4). Assuming such a distribution and by allowing the growth rate of the guiding radius to vary, we tested several models to fit the data (figure 5). The best among them is a model whose guiding centre moves along the surface trace of the fault plane with rupture expanding unilaterally in a horizontal direction (figure 6). This model suggests that the observed-non-uniform speed of creep propagation is probably real and not due to geometric effects.

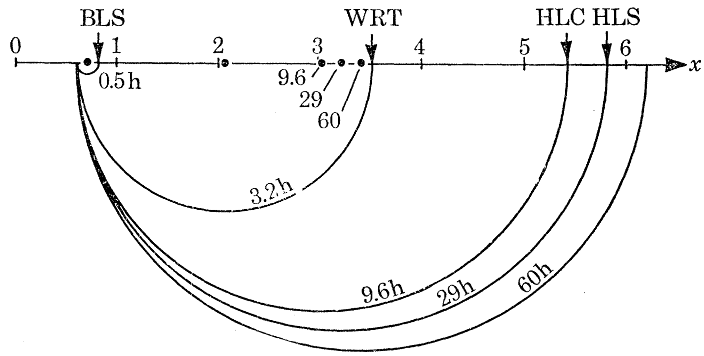

FIGURE 6. Fault-plane view of a theoretical faulting model that can reasonably fit the creep data of the 17 July 1971 event (case $h = 0$ in figure 5). The fault trace is along the x-axis, below which is the fault plane. The rupture expands with a circular boundary whose positions are shown for several specified times.

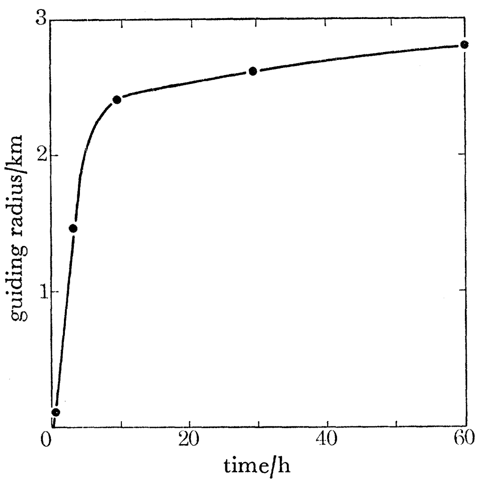

FIGURE 7. Guiding radius as function of time for the 17 July 1971 event.

The slowing down of the creep process is also indicated in its slip velocity, which is lower near the end of the event (at HLS) than near the beginning (at BLS). This feature is also shown in two other events (11 July 1971 in figure 3*a* and 30 July 1970 in figure 2). This difference is particularly obvious in the creep curves recorded at BLS for the two July 1971 events since this station is located near the end of one event but the beginning of the other.

Figure 7 shows how the model guiding radius for the 17 July 1971 event grows with time. The final rupture length according to this model is 5.6 km.

The observed creep curves have precursors that do not exist in the model curves (figure 5). These precursors may be strain changes associated with the propagating rupture front. Such changes should be larger for stations nearer the end of the rupture zone, as is observed, since rupture, when approaching such stations, has larger dimension and offset. If this interpretation is correct, then the extensional strain in the 45° diagonal at the rupture front is as high as 4.5×10^{-5} (at HLS). For comparison, figure 8 shows theoretical curves of this strain component for a propagating vertical edge dislocation of a slip strength equal to 10^{-6} times its distance from the rupture origin, calculated according to an expression given by Frank (1973).

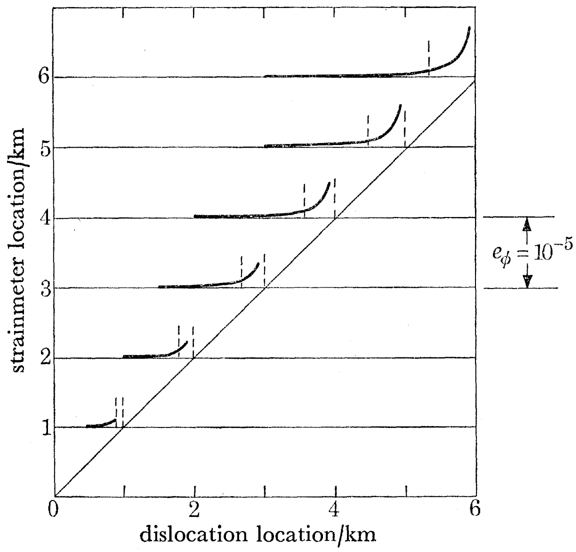

FIGURE 8. Theoretical strain records (extension in 45° diagonal) at several different locations on the fault trace for a propagating vertical edge dislocation of increasing slip strength. The dashed lines indicate the range in which the strain exceeds 10^{-6} proir to the rupture arrival.

DISCUSSION

It is well known that fault creep does not generate observable seismic waves. It appears from this study that the low seismic excitation of the creep process is a result of its extreme slowness in particle motion, not of smallness in strain energy release. The large 17 July 1971 creep event has a rupture length and an offset comparable to those of a shallow earthquake of magnitude 4.7 (King & Knopoff 1968).

The offsets of creep events are, on the average, an order of magnitude smaller than those of shallow earthquakes of comparable rupture length, as observed earlier (King *et al.* 1970). This result implies that the strain change associated with a creep event is an order of magnitude smaller accordingly.

REFERENCES (King *et al.*)

Frank, F. C. 1973 *Phil. Trans. R. Soc. Lond.* A **274**, 351 (this volume).
King, C.-Y. 1970 *Bull. seism. Soc. Am.* **60**, 491–501.
King, C.-Y. 1972 *Bull. seism. Soc. Am.* **62**, 551–559.
King, C.-Y. & Knopoff, L. 1968 *Bull. seism. Soc. Am.* **58**, 249–257.
King, C.-Y., Nason, R. D. & Tocher, D. 1970 *Earthq. Res. in ESSA*, 1969–1970, *ESSA Tech Rep.* **ERL 182–ESL 11**, 15–18.
Nason, R. D. 1970 *Earthq. Res. in ESSA*, 1969–70, *ESSA*, *Tech. Rep.* **ERL 182–ESL 11**, 12–15.
Nason, R. D. 1971 Ph.D. Thesis, University of Californian, San Diego, 231 pp.
Steinbrugge, K. V. & Zacher, E. G. 1960 *Bull. seism. Soc. Am.* **50**, 389–396.
Tocher, D. 1960 *Bull. seism. Soc. Am.* **50**, 396–404.